# Magnetic oscillations in planar systems with the Dirac-like spectrum of quasiparticle excitations. II. Transport properties

V. P. Gusynin[1,*] and S. G. Sharapov[2,†]
[1]*Bogolyubov Institute for Theoretical Physics, Metrologicheskaya Str. 14-b, Kiev 03143, Ukraine*
[2]*Istituto Nazionale per la Fisica della Materia (INFM), Institute for Scientific Interchange, via Settimio Severo 65, I-10133 Torino, Italy*
(Received 3 December 2004; published 24 March 2005)

The quantum magnetic oscillations of electrical (Shubnikov–de Haas effect) and thermal conductivities are studied for graphene which represents a distinctive example of planar systems with a linear, Dirac-like spectrum of quasiparticle excitations. We show that if utmost care is taken to separate electron and phonon contributions in the thermal conductivity, the oscillations of electron thermal conductivity $\kappa(B)$ and Lorenz number, $L(B)$ would be observable in the low-field (less than a few teslas) regime.

DOI: 10.1103/PhysRevB.71.125124 PACS number(s): 71.70.Di, 73.43.Qt, 11.10.Wx

## I. INTRODUCTION

There is a variety of condensed matters systems that in the first approximation can be regarded as planar and which in the low-energy sector can be described by the Dirac-like form of the effective Hamiltonian. The difference in the behavior of the particles with the usual parabolic spectrum and the linear, Dirac-like spectrum becomes particularly prominent when an external quantizing magnetic field $B$ is applied perpendicularly to the plane. The energies of Landau levels for free nonrelativistic electrons are $E_n = e\hbar B/(mc)\left(n+\frac{1}{2}\right)$, while for the "relativistic" problem

$$E_n = \sqrt{e\hbar v_F^2 B 2n/c}, \tag{1}$$

with $n=0,1,\ldots$. Here $e$ is the electron charge, $m$ is the effective mass of carriers in the parabolic band, $v_F$ is the Fermi velocity of the system with linear dispersion, and we wrote $\hbar$ and $c$ explicitly; in the following sections we set $\hbar = c = k_B = 1$, unless stated explicitly otherwise.

The most important qualitative difference between these two spectrums is that for the realistic values of the parameters $m$ and $v_F$ rather weak fields $B \sim 10$ T are sufficient to drive "relativistic" systems in the extreme quantum regime[1] causing such interesting phenomena as quantum magnetoresistance. Another qualitatively distinguishable feature of the Dirac-like quasiparticles is an unusual form of the semiclassical quantization condition for energy levels in the magnetic field, $S(\epsilon) = 2\pi eB/(\hbar c)(n+\gamma)$, where $S$ is the cross-sectional area of the orbit in $\mathbf{k}$ space, $n$ is a large integer ($n > 0$), and $\gamma$ is constant ($0 \leqslant \gamma \leqslant 1$). For the parabolic dispersion $\gamma = 1/2$, which is commonly used in describing magnetic oscillation (MO) phenomena in metals,[2] so that the corresponding Berry's phase $\gamma - 1/2$ is zero. However, for the Dirac quasiparticles Berry's phase is nontrivial[3] and $\gamma = 0$, so that the commonly used expressions[2] have to be modified accordingly. This was indeed obtained in our previous paper,[4] where we have studied MO of the density of states (DOS), thermodynamic potential, and magnetization in $\mathrm{QED}_{2+1}$ with the spectrum (1). We have also discussed the underlying condensed matter models and systems that in the low-energy approximation are reduced to $\mathrm{QED}_{2+1}$ form. Among them is graphite, which is probably the most promising and convenient for experimental investigation of the ultraquantum regime, when only a few lowest Landau levels are occupied. This semimetal was originally studied almost 50 years ago, and there was a considerable renewal of the interest in the electronic properties of this material during the past decade due to the discovery of novel carbon-based materials such as carbon nanotubes constructed from wrapped graphene sheets.[5] While graphite itself is a three-dimensional material in which planar sheets of carbon atoms are stacked, graphene is an individual layer or sheet made from the carbon atoms.

The simplified $\mathrm{QED}_{2+1}$ description is obviously appropriate for graphene. In Kish graphite the anisotropy of the resistivity $\rho_c$ along the $c$-axis direction and the basal-plane resistivity $\rho_b$ can be $\rho_c/\rho_b \sim 10^2$ and even as large as $\rho_c/\rho_b \sim 5\times 10^4$ in highly oriented pyrolytic graphite (HOPG),[6] indicating that the layers are weakly coupled. Therefore in the first approximation, the $\mathrm{QED}_{2+1}$ description with some limitations may also be used for graphite. Indeed, early theoretical investigations of graphite show that while low-lying Landau levels correspond to Eq. (1), there are other levels related to the warping of the graphite Fermi surface.[7] Very recent measurements of de Haas–van Alphen (dHvA) and Shubnikov–de Haas (SdH) oscillations in HOPG (Ref. 8) (for earlier literature see Refs. 9 and 10) confirm that among other carriers in graphite there is a majority of holes with two-dimensional (2D) Dirac-like spectrum. The dependences of the thermal and Hall conductivities on the applied magnetic field in HOPG were studied in Ref. 11 and more comprehensive data on thermal conductivity and the deviations from the Wiedemann-Franz (WF) law were reported in Ref. 12. We mention also recent STS observations[13] of Landau levels at graphite surfaces. Finally we refer to monocrystalline graphitic films made by repeated peeling of small mesas of HOPG.[14] These films contain only a few layers of graphene. The SdH oscillations are clearly observed in this material[14] and they depend only on the perpendicular component of the applied magnetic field. This proves the 2D nature of the material. Moreover, the carrier density (and even the character of carriers, either electrons or holes) in this system is controllable by electric-field doping, so that there are SdH oscillations with varying applied voltage.[15]

The purpose of the present paper is to extend the analysis of our previous paper[4] and study the MO of the electrical, $\sigma(B)$ (SdH effect), and thermal $\kappa(B)$ conductivities. We dem-

 

onstrate that since the field dependences of $\sigma(B)$ and $\kappa(B)$ at low but still finite temperatures are different, there is a violation of the WF law with observable oscillations of the Lorenz number

$$L(B,T) \equiv \frac{\kappa(B,T)}{\sigma(B,T)T}. \tag{2}$$

We begin by presenting in Sec. II the model Lagrangian describing Dirac quasiparticles in graphene. The general expressions for electrical and thermal conductivities are written in terms of the same spectral function $\mathcal{A}(B)$ and the thermal conductivity is considered also including the thermal power term. In Sec. III we analytically extract magnetic oscillations contained in the spectral function $\mathcal{A}(B)$. In the Discussion, Sec. IV, our final results are summarized and their applicability for the graphite is considered.

## II. MODEL AND GENERAL EXPRESSIONS FOR ELECTRICAL AND THERMAL CONDUCTIVITIES

### A. Model Lagrangian

The Lagrangian density of noninteracting quasiparticles in a single graphene sheet in the continuum limit reads (see, e.g., Refs. 16 and 17)

$$\mathcal{L}_0 = \sum_{\sigma=\pm1} v_F \overline{\Psi}_\sigma(t,\mathbf{r}) \Bigg[ \frac{i\gamma^0(\partial_t - i\mu_\sigma)}{v_F} - i\gamma^1(\partial_x - ieA_x) - i\gamma^2(\partial_y - ieA_y) \Bigg] \Psi_\sigma(t,\mathbf{r}), \tag{3}$$

where the four-component Dirac spinor $\Psi_\sigma=(\psi_{1\sigma},\psi_{2\sigma})$ is combined from two spinors $\psi_{1\sigma}$, $\psi_{2\sigma}$ that describe the Bloch states residing on the two different sublattices of the biparticle hexagonal lattice of the graphene sheet, and $\sigma=\pm1$ is the spin. In Eq. (3), $\overline{\Psi}_\sigma=\Psi_\sigma^\dagger\gamma^0$ is the Dirac-conjugated spinor and $4\times4$ $\gamma$ matrices are either $(\sigma_3, i\sigma_3, -i\sigma_1)\otimes\sigma_3$ (Ref. 18) or their unitary-equivalent representation can be taken from Refs. 16 and 19.

Note that there is no principal difference between two-band models for electron and holes discussed in Refs. 20 and 21 and a model with Dirac fermions, where these electron and holes with identical velocities are built in the formalism. There are, however, some cases like a double-resonant Raman scattering in graphite,[22] where the asymmetry between the bonding, $E=v_F|\mathbf{k}|$, and antibonding, $E=-v_F'|\mathbf{k}|$, bands in graphite is essential, so that multiband models are more suitable.

Since the terms with $\partial_{x,y}$ in Eq. (3) originate from the usual kinetic term of the tight-binding Hamiltonian, vector potential $\mathbf{A}$ is inserted in the Lagrangian (3) using a minimal coupling prescription. The vector potential for the external magnetic field $\mathbf{B}$ perpendicular to the plane is taken in the symmetric gauge

$$\mathbf{A} = \left( -\frac{B}{2}x_2, \frac{B}{2}x_1 \right). \tag{4}$$

Using for the value of the nearest-neighbor hopping matrix element of graphite $t\sim2.3$ eV, we obtain the Fermi velocity of $v_F\approx7.4\times10^5$ m/s, and accordingly one can estimate from Eq. (1) that $E_1\sim300\ \mathrm{K}\times\sqrt{B\ [\mathrm{T}]}$.

Since the Lagrangian (3) originates from nonrelativistic many-body theory, the interaction of the spin degree of freedom with magnetic field

$$\mathcal{L}_B = \mu_B B \sum_{\sigma=\pm} \sigma \overline{\Psi}_\sigma(t,\mathbf{r})\gamma^0\Psi_\sigma(t,\mathbf{r}) \tag{5}$$

has to be explicitly included by considering spin splitting $\mu_\sigma=\mu-\sigma\mu_B B$ Ref. 2 of the chemical potential $\mu$, where $\mu_B=e\hbar/(2mc)$ is the Bohr magneton. Note that the number of spin components can be regarded as an additional adjustable flavor index of fermions $\sigma=1,\ldots,N$ and $N=2$ corresponds to the physical case. The magnitude of the Zeeman term depends on the ratio $\mu_B/k_B\simeq0.67\ \mathrm{K\ T^{-1}}$. This term, in fact, has the same magnitude as the distance between Landau levels in the nonrelativistic problem. Although we will include this term for completeness in the analytical expressions, in the numerical calculations it can be safely neglected because it is much smaller than estimated above $E_1$.

To make the treatment more general, we also include a mass (gap) term

$$\mathcal{L}_\Delta = \sum_{\sigma=\pm1} \overline{\Psi}_\sigma(t,\mathbf{r})\Delta\Psi_\sigma(t,\mathbf{r}), \tag{6}$$

in the Lagrangian (3). For example, it is well known that an external magnetic field is a strong catalyst in generating such a gap for Dirac fermions (the phenomenon of magnetic catalysis).[23] Usually the opening of the gap marks an important transition which occurs in the system. In particular, in the case of pyrolytic graphite a poor screening of the Coulomb interaction may lead to excitonic instability, resulting in the opening of the gap in the electronic spectrum and manifesting itself through the onset of an insulating charge density wave (see, e.g., Refs. 18, 19, and 24).

### B. Electrical conductivity

The dc conductivity tensor can be found using Kubo formula[25]

$$\sigma_{ij} = -\lim_{\Omega\to0} \frac{\mathrm{Im}\Pi_{ij}^R(\Omega+i0)}{\Omega}, \tag{7}$$

where $\Pi_{ij}^R(\Omega)$ is the retarded current-current correlation function (see, e.g., Refs. 19 and 26)

$$\Pi_{ij}^R(\Omega+i0) = \frac{e^2v_F^2}{2}\sum_\sigma \int_{-\infty}^{\infty} d\omega_1 d\omega_2 \times \frac{\tanh[(\omega_2-\mu_\sigma)/2T] - \tanh[(\omega_1-\mu_\sigma)/2T]}{\omega_1-\omega_2+\Omega+i0} \times \int \frac{d^2k}{(2\pi)^2} \mathrm{tr}[A(\omega_1,\mathbf{k})\gamma_i A(\omega_2,\mathbf{k})\gamma_j]. \tag{8}$$

Here $A(\omega,\mathbf{k})$ is the spectral function associated with the translationary-invariant part of the Green's function of Dirac

quasiparticles in an external magnetic field given by Eqs. (3.3) and (3.6) of Ref. 4 (see also Refs. 19, 23, and 26). Then for the diagonal conductivity $\sigma=\sigma_{xx}=\sigma_{yy}$ we have

$$\sigma = \pi e^2 v_F^2 \sum_\sigma \int \frac{d^2k}{(2\pi)^2} \int_{-\infty}^{\infty} d\omega [-n_F'(\omega-\mu_\sigma)] \times \mathrm{tr}[A(\omega,\mathbf{k})\gamma_1 A(\omega,\mathbf{k})\gamma_1], \tag{9}$$

where $-n_F'(\omega-\mu)=(1/4T)\cosh^{-2}[(\omega-\mu)/2T]$ is the derivative of the Fermi distribution. Further details of calculation of tr and the momentum integral in Eq. (9) were considered in Refs. 19, 26, and 27, so here we write down a rather simple final expression for the electrical conductivity in an external magnetic field:

$$\sigma = e^2 \sum_\sigma \int_{-\infty}^{\infty} \frac{d\omega}{4T\cosh^2\dfrac{\omega-\mu_\sigma}{2T}} \mathcal{A}(\omega,B,\Gamma,\Delta), \tag{10}$$

where the function

$$\mathcal{A}(\omega,B,\Gamma,\Delta) = \frac{1}{\pi^2}\frac{\Gamma^2}{(eB)^2+(2\omega\Gamma)^2} \times \left\{ 2\omega^2 + \frac{(\omega^2+\Delta^2+\Gamma^2)(eB)^2 - 2\omega^2(\omega^2-\Delta^2+\Gamma^2)eB}{(\omega^2-\Delta^2-\Gamma^2)^2+4\omega^2\Gamma^2} - \frac{\omega(\omega^2-\Delta^2+\Gamma^2)}{\Gamma}\mathrm{Im}\psi\left(\frac{\Delta^2+\Gamma^2-\omega^2-2i\omega\Gamma}{2eB}\right)\right\}. \tag{11}$$

Here, in order to consider the MO for a more realistic case, we introduced the effect of quasiparticle scattering by making $\delta$-like quasiparticle peaks associated with the Landau levels Lorentzians with a constant energy-independent width $\Gamma$ (see details in Ref. 4). This approximation still allows us to derive a rather simple analytical expression, Eq. (11), where $\psi$ is the digamma function, which eventually results in a *Dingle* factor in the expression for the amplitude of MO.

Note that in general one should consider dressed fermion propagators that include the self-energy $\Sigma(\omega)$ due to the scattering from impurities. Up to now the problem of scattering from impurities in the presence of a magnetic field does not have yet a satisfactory solution. Therefore, here we have chosen the case of constant width $\Gamma=\Gamma(\omega=0)=-\mathrm{Im}\Sigma^R(\omega=0)=1/(2\tau)$, $\tau$ being the mean free time of quasiparticles.

Such a Lorentzian broadening of Landau levels with a constant $\Gamma$ was found to be a rather good approximation valid in not very strong magnetic fields.[2,28] Definitely, the treatment of disorder in the presence of the magnetic field in such a simplified manner should be considered as only a first step until further progress in this problem is achieved (in connection with this, see Refs. 29 and 30).

### C. Thermal conductivity

The longitudinal thermal conductivity can also be calculated using a thermal Kubo formula[25]

$$\frac{\kappa(B,T)}{T} = -\frac{1}{T^2}\lim_{\Omega\to 0}\frac{\mathrm{Im}\Pi_{EE}^R(\Omega+i0)}{\Omega} - \frac{1}{T^2\sigma}\lim_{\Omega\to 0}\frac{[\mathrm{Im}\Pi_{EC}^R(\Omega+i0)]^2}{\Omega^2}. \tag{12}$$

Here $\Pi_{EE}^R(\Omega)$ is the retarded longitudinal energy current-current correlation function and $\Pi_{EC}^R(\Omega)$ is the retarded longitudinal correlation function of energy current with electrical current and the expression for the energy current operator is given in Refs. 26 and 27.

We note in passing that the second term of Eq. (12) is related to the thermal power

$$S = -\frac{1}{T}\lim_{\Omega\to 0}\frac{\mathrm{Im}\Pi_{EC}^R(\Omega+i0)}{\mathrm{Im}\Pi^R(\Omega+i0)}, \tag{13}$$

where $\Pi^R(\Omega+i0)=\Pi_{xx}^R(\Omega+i0)=\Pi_{yy}^R(\Omega+i0)$. The presence of the thermal power term in Eq. (12) ensures that the energy current is evaluated under the condition of vanishing electrical current.[25]

Similarly to the above-derived electrical conductivity we finally arrive at

$$\frac{\kappa(B,T)}{T} = \sum_\sigma \int_{-\infty}^{\infty} d\omega \left(\frac{\omega-\mu_\sigma}{T}\right)^2 \frac{1}{4T\cosh^2\dfrac{\omega-\mu_\sigma}{2T}} \times \mathcal{A}(\omega,B,\Gamma,\Delta) - \frac{e^2}{\sigma(B,T)} \times \left[\sum_\sigma \int_{-\infty}^{\infty} d\omega \frac{\omega-\mu_\sigma}{T}\frac{1}{4T\cosh^2\dfrac{\omega-\mu_\sigma}{2T}}\mathcal{A}(\omega,B,\Gamma,\Delta)\right]^2, \tag{14}$$

where $\mathcal{A}$ is the same function (11) as for the electrical conductivity. This function contains all information about the field dependence of the transport properties of the systems with a linear dispersion law, including the MO. While the representation (11) can already be used for numerical calculations, for analytical work it is useful to extract explicitly the MO that are contained in the digamma function $\psi$ when the real part of its argument becomes negative.

## III. ANALYTICAL CONSIDERATION OF OSCILLATIONS

### A. Extracting oscillations from $\mathcal{A}$ using $\psi$-function properties

The oscillations of $\mathcal{A}$ in $1/B$ can be extracted using the relationship for $\psi$ function,

$$\psi(-z) = \psi(z) + \frac{1}{z} + \pi\cot\pi z, \tag{15}$$

which [see also Eq. (4.18) of Ref. 4] results in the expression

$$\psi\left(\frac{\Delta^2-(\epsilon+i\Gamma)^2}{2eB}\right)$$
$$=\psi\left(\frac{\Delta^2-(\epsilon+i\Gamma)^2}{2eB}\right)[\theta(\epsilon^2-\Delta^2-\Gamma^2)+\theta(\Delta^2+\Gamma^2-\epsilon^2)]$$
$$=\mathrm{Re}\,\psi\left(\frac{|\epsilon^2-\Delta^2-\Gamma^2|-2i\epsilon\Gamma}{2eB}\right)$$
$$-i\,\mathrm{sgn}(\epsilon^2-\Delta^2-\Gamma^2)\mathrm{Im}\psi\left(\frac{|\epsilon^2-\Delta^2-\Gamma^2|-2i\epsilon\Gamma}{2eB}\right)$$
$$+\theta(\epsilon^2-\Delta^2-\Gamma^2)\left[\frac{2eB}{\epsilon^2-\Delta^2-\Gamma^2+2i\epsilon\Gamma}\right.$$
$$\left.+\pi\cot\pi\frac{\epsilon^2-\Delta^2-\Gamma^2+2i\epsilon\Gamma}{2eB}\right]. \tag{16}$$

Taking the imaginary part of the last equation, we obtain

$$\mathrm{Im}\psi\left(\frac{\Delta^2-(\omega+i\Gamma)^2}{2eB}\right)$$
$$=-\mathrm{sgn}(\omega^2-\Delta^2-\Gamma^2)\mathrm{Im}\psi\left(\frac{|\omega^2-\Delta^2-\Gamma^2|-2i\omega\Gamma}{2eB}\right)$$
$$-\theta(\omega^2-\Delta^2-\Gamma^2)\left[\frac{4eB\omega\Gamma}{(\omega^2-\Delta^2-\Gamma^2)^2+4\omega^2\Gamma^2}\right.$$
$$\left.+\pi\frac{\sinh(2\pi\omega\Gamma/eB)}{\cosh(2\pi\omega\Gamma/eB)-\cos[\pi(\omega^2-\Delta^2-\Gamma^2)/eB]}\right]. \tag{17}$$

Then substituting Eq. (17) in Eq. (11) we obtain

$$\mathcal{A}(\omega,B,\Gamma,\Delta)$$
$$=\frac{1}{\pi^2}\frac{\Gamma^2}{(eB)^2+(2\omega\Gamma)^2}\left\{2\omega^2+\frac{(eB)^2/2}{(\omega+\Delta)^2+\Gamma^2}\right.$$
$$+\frac{(eB)^2/2}{(\omega-\Delta)^2+\Gamma^2}-\frac{2\omega^2(\omega^2-\Delta^2+\Gamma^2)eB}{(\omega^2-\Delta^2-\Gamma^2)^2+4\omega^2\Gamma^2}$$
$$+\frac{\omega(\omega^2-\Delta^2+\Gamma^2)}{\Gamma}\left[\mathrm{sgn}(\omega^2-\Delta^2-\Gamma^2)\right.$$
$$\times\mathrm{Im}\psi\frac{(|\omega^2-\Delta^2-\Gamma^2|2i\omega\Gamma)}{2eB}$$
$$+\theta(\omega^2-\Delta^2-\Gamma^2)\left(\frac{4eB\omega\Gamma}{(\omega^2-\Delta^2-\Gamma^2)^2+4\omega^2\Gamma^2}\right.$$
$$\left.\left.\left.+\pi\frac{\sinh(2\pi\omega\Gamma/eB)}{\cosh(2\pi\omega\Gamma/eB)-\cos[\pi(\omega^2-\Delta^2-\Gamma^2)/eB]}\right)\right]\right\}, \tag{18}$$

where the oscillations are contained in the last term of Eq. (18). Note that the real part of the argument of $\psi$ function in Eq. (18) is already positive and the signs before $\psi$ in Eqs. (11) and (18) are different.

For $\omega^2>\Delta^2+\Gamma^2$ using the relationship

$$\mathrm{Re}\frac{e^{-(a-ib)}}{1-e^{-(a-ib)}}=\frac{\cos b-e^{-a}}{2(\cosh a-\cos b)}, \tag{19}$$

one can expand

$$\frac{\sinh(2\pi|\omega|\Gamma/eB)}{\cosh(2\pi\omega\Gamma/eB)-\cos[\pi(\omega^2-\Delta^2-\Gamma^2)/eB]}$$
$$=1+2\sum_{k=1}^{\infty}\cos[\pi k(\omega^2-\Delta^2-\Gamma^2)/eB]\exp(-2\pi k|\omega|\Gamma/eB) \tag{20}$$

and finally arrive at the expression for oscillatory part of $\mathcal{A}$:

$$\mathcal{A}_{\mathrm{osc}}(\omega,B,\Gamma,\Delta)=\frac{2}{\pi}\frac{\omega\Gamma(\omega^2-\Delta^2+\Gamma^2)\theta(\omega^2-\Delta^2-\Gamma^2)}{(eB)^2+(2\omega\Gamma)^2}$$
$$\times\sum_{k=1}^{\infty}\cos\frac{\pi k(\omega^2-\Delta^2-\Gamma^2)}{eB}$$
$$\times\exp\left(-\frac{2\pi k|\omega|\Gamma}{eB}\right). \tag{21}$$

#### *1. Low-field nonoscillatory limit*

Equation. (18) can be simplified in the low-field limit:

$$\mathcal{A}(\omega,B,\Gamma,\Delta)$$
$$=\frac{1}{2\pi^2}\left[1-\frac{\omega^2-\Delta^2+\Gamma^2}{2|\omega|\Gamma}\mathrm{sgn}(\omega^2-\Delta^2-\Gamma^2)\right.$$
$$\times\arctan\frac{2|\omega|\Gamma}{|\omega^2-\Delta^2-\Gamma^2|}+\theta(\omega^2-\Delta^2-\Gamma^2)$$
$$\times\frac{\pi(\omega^2-\Delta^2+\Gamma^2)}{2\omega\Gamma}$$
$$\left.\times\frac{\sinh(2\pi\omega\Gamma/eB)}{\cosh(2\pi\omega\Gamma/eB)-\cos[\pi(\omega^2-\Delta^2-\Gamma^2)/eB]}\right], \tag{22}$$

where we kept $B$ only in the oscillatory part of $\mathcal{A}$. For $\omega^2<\Delta^2+\Gamma^2$ after using the relationship

$$\arctan x=\frac{\pi}{2}-\arctan\frac{1}{x},\quad x>0, \tag{23}$$

the last equation reduces to [see also Eq. (4.16) of Ref. 26]

$$\mathcal{A}(\omega,B=0,\Gamma,\Delta)=\frac{1}{2\pi^2}\left[1+\frac{\omega^2-\Delta^2+\Gamma^2}{2|\omega|\Gamma}\right.$$
$$\left.\times\left(\frac{\pi}{2}-\arctan\frac{\Delta^2+\Gamma^2-\omega^2}{2|\omega|\Gamma}\right)\right]. \tag{24}$$

### B. Oscillating parts of electrical and thermal conductivities

Substituting Eq. (21) in Eq. (10) one can obtain the expression for oscillating part of conductivity:

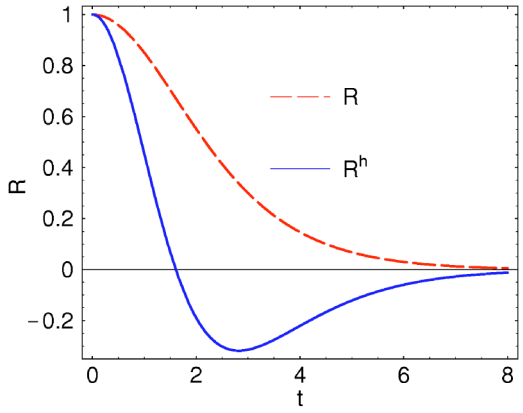


FIG. 1. (Color online) The temperature amplitude factors $R_T(t)$ and $R_T^h(t)$ given by Eqs. (26) and (30).

$$\sigma_{\rm osc} = \frac{4e^2|\mu|\Gamma}{\pi}\frac{(\mu^2-\Delta^2+\Gamma^2)\theta(\mu^2-\Delta^2-\Gamma^2)}{(eB)^2+(2\mu\Gamma)^2} \times\sum_{k=1}^{\infty}\cos\left[\frac{\pi k(\mu^2-\Delta^2-\Gamma^2)}{eB}\right]R_T(k,\mu)R_D(k,\mu), \tag{25}$$

where we introduced the *temperature amplitude* factor

$$R_T(k,\mu)\equiv R_T(t_k)=\frac{t_k}{\sinh t_k},\quad t_k=\frac{2\pi^2kT\mu}{eB}\quad [R_T(0)=1], \tag{26}$$

and the *Dingle factor*

$$R_D(k,\mu)=\exp\left[-\frac{2\pi k|\mu|\Gamma}{eB}\right]. \tag{27}$$

Deriving Eq. (25) we made the following simplifying assumptions: (i) Spin splitting is not included, and (ii) the low-temperature $T\to 0$ limit is considered. Thus after making a shift $\omega\to\omega+\mu$ and changing the variable $\omega\to 2T\omega$, and keeping only the linear in $T$ terms in the oscillating part of the integrand, we used the integral

$$\int_0^\infty dx\frac{\cos bx}{\cosh^2 x}=\frac{\pi b/2}{\sinh \pi b/2} \tag{28}$$

to obtain the temperature amplitude factor (26). It is essential that in contrast to the the Dingle and temperature factors for nonrelativisitic spectrum both Eqs. (26) and (27) factors for the relativistic spectrum contain chemical potential $\mu$ (see also Ref. 4). The distinctive concentration dependence of $R_T$ should be observed experimentally.

Similarly to Eq. (25) one arrives at the expression for the oscillating part of thermal conductivity (14):

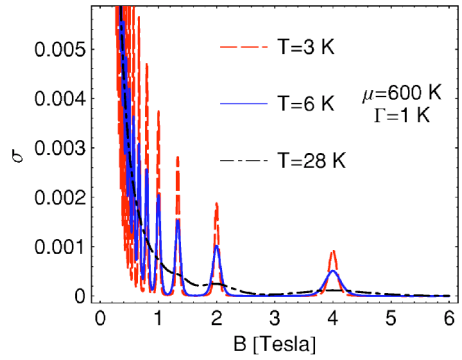


FIG. 2. (Color online) The normalized conductivity $\sigma(B,T)/\sigma(B=0,T)$ as a function of field $B$ for three different values of temperature $T$ for $\mu=600$ K and $\Gamma=1$ K. We use $eB\to(4.5\times10^4\ \mathrm{K}^2)B$ (T).

$$\frac{\kappa_{\rm osc}}{T} = \frac{4\pi|\mu|\Gamma}{3}\frac{(\mu^2-\Delta^2+\Gamma^2)\theta(\mu^2-\Delta^2-\Gamma^2)}{(eB)^2+(2\mu\Gamma)^2} \times\sum_{k=1}^{\infty}\cos\left[\frac{\pi k(\mu^2-\Delta^2-\Gamma^2)}{eB}\right]R_T^h(k,\mu)R_D(k,\mu), \tag{29}$$

where

$$R_T^h(t_k)=\frac{12}{\pi^2}\frac{d^2R_T(t_k)}{dt_k^2} =\frac{6}{\sinh t_k}\left[\coth t_k-\frac{t_k}{2}-\frac{t_k}{\sinh^2 t_k}\right]\quad [R_T^h(0)=1] \tag{30}$$

is the *temperature amplitude* factor for thermal conductivity obtained using the second derivative of the integral (28). The temperature amplitude factors $R_T(t)$ and $R_T^h(t)$ are shown in

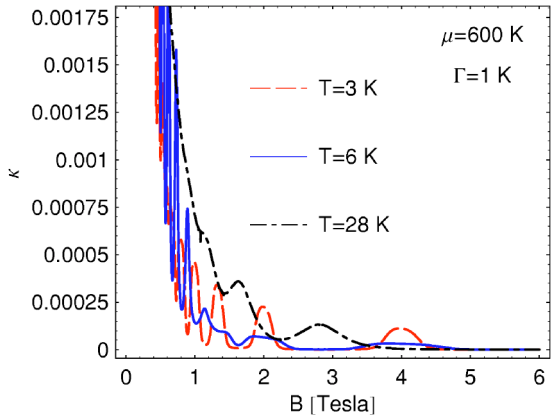


FIG. 3. (Color online) The normalized thermal conductivity $\kappa(B,T)/\kappa(B=0,T)$ as a function of field $B$ for three different values of temperature $T$ for $\mu=600$ K and $\Gamma=1$ K. We use $eB\to(4.5\times10^4\ \mathrm{K}^2)B$ (T).

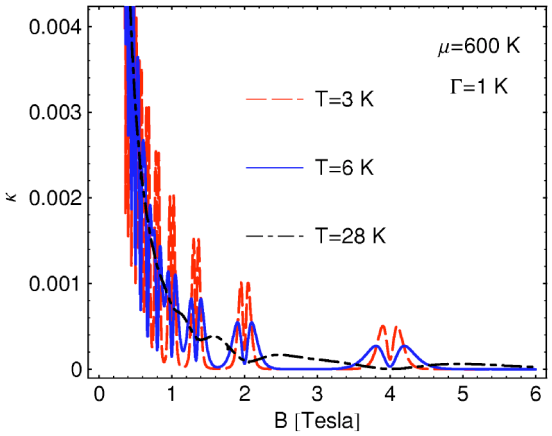


FIG. 4. (Color online) The normalized thermal conductivity $\kappa_0(B,T)/\kappa(B=0,T)$ [calculated without the second term of Eq. (12) that originates from the condition of absence electrical current in the system] as a function of field $B$ for three different values of temperature $T$ for $\mu=600$ K and $\Gamma=1$ K. We use $eB\rightarrow(4.5\times10^4\mathrm{K}^2)B$ (T).

Fig. 1. Interestingly the dependence $R_T^h(t)$ is nonmonotonic and $R_T^h(t)$ even changes its sign.

## IV. DISCUSSION

Based on Eqs. (10) and (14) in Figs. 2–5 we compute the field dependences of $\sigma(B,T)/\sigma(B=0,T)$ and $\kappa(B,T)/\kappa(B=0,T)$ and the normalized Lorenz number $L(B,T)/L_0$, where $L_0=\pi^2k_B^2/(3e^2)$ is Sommerfeld's value for the Lorenz ratio. To simplify our consideration we set $\Delta=0$, but it may be necessary and quite interesting to consider the influence of $\Delta$ on MO; see Ref. 4. As mentioned above Eq. (6), we also do not include spin splitting. By analyzing these figures one can conclude the following.

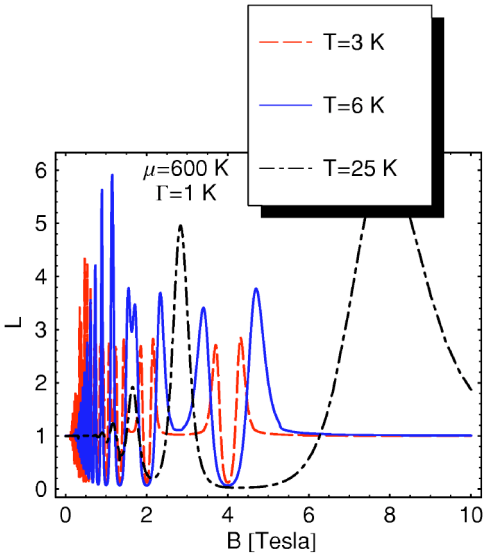


FIG. 5. (Color online) The normalized Lorenz number $L(B,T)/L_0$ as a function of field $B$ for three different values of temperature $T$ for $\mu=600$ K and $\Gamma=1$ K. We use $eB\rightarrow(4.5\times10^4\ \mathrm{K}^2)B$ (T).

(i) As usual, the conditions favorable for the magnetic oscillations are $\Gamma,T\ll\omega_L$, where $\omega_L\sim E_1$ is the distance between Landau levels. This regime is different from the regime $\Gamma\ll\omega_L\ll T$ of an unconventional magnetotransport[21] when MO's are still not resolved due to the thermal smearing of Landau levels.

(ii) As the field increases from $B=0$ both electrical and thermal conductivities decrease rapidly and start to oscillate when Landau levels cross the Fermi surface. The specific of graphene is that for the realistic values of the parameters there are only a few Landau levels below the Fermi surface. As the field $B$ increases, these levels quickly cross the Fermi surface, and as one can see from Fig. 2 for $B>4$ $T$ the lowest Landau level $E_1$ is already above the Fermi surface so that the MO's disappear and the system can, in principle, enter in the quantum Hall effect regime. Thus MO's in graphene with $eB\lesssim\mu^2$ are quite different from the conventional MO's when there are so many Landau levels below the Fermi surface that $\omega_L\ll\mu$ and when a new level crosses the Fermi surface the system returns practically in the same state as before.

For Dirac fermions in order to have at least one oscillation the inequality [see Eq. (8.20) of Ref. 4] $\mu^2-\Delta^2\geqslant 2eB$ have to be satisfied, and analyzing the experimental data of Refs. 8 and 11 there is a temptation to distinguish there the regimes of conventional MO's and quantum Hall effect. However, the real situation is more involved due to the difference between the model for graphene with linearized spectrum and measured properties of bulk graphite (see also Ref. 13). Nevertheless, observation of the plateaulike features in the Hall resistivity for $B\gtrsim 2$ T (Ref. 11) suggests that for these fields the system is already in the quantum Hall effect regime.

(iii) Comparing Figs. 2 and 3, one can see that $\sigma(B)$ and $\kappa(B)$ do not oscillate in phase. In particular, we observe that at $T=28$ K the oscillations of $\sigma(B)$ are practically invisible, while one can still notice some oscillations of $\kappa(B)$.

To look closer at the difference between $\sigma$ and $\kappa$ in Fig. 4 we also plotted the thermal conductivity $\kappa_0(B,T)$ calculated without the second term of Eq. (12). In normal metals this second term is considered to be unimportant because usually it is $\sim T^2/\mu^2$ times less than the first term of Eq. (12) and because the WF law is always considered in the limit $T\ll\mu$ this term is usually neglected.

(iv) By comparing Figs. 2 and 4, it is easy to see that each peak of the electrical conductivity is accompanied by two satellite peaks of the thermal conductivity. The dip between these two peaks in $\kappa(B)$ coincides with the peak of $\sigma(B)$. The origin of these satellite peaks is related to the fact that the expression for the thermal conductivity (12) contains the factor $g(\omega)=-n_F'(\omega-\mu)(\omega-\mu)^2/T^2$ and thus measures $\mathcal{A}(\omega,B,\Gamma)$ below and above the Fermi energy, while the electrical conductivity probes $\mathcal{A}(\omega,B,\Gamma)$ *at* the Fermi energy, because it contains just the factor $n_F'(\omega)$ (see Ref. 31 and Figs. 12 and 13 of Ref. 26).

(v) Let us now compare Figs. 3 and 4. At $T=3$ K each double-peak structure observed in Fig. 4 is replaced by a single broader peak in Fig. 3. This reflects the fact that the

full expression (12) for $\kappa(B) \sim \kappa_0(B) - a(B)/\sigma(B)$, so that if the coefficient $a(B)$ is large enough, the peaks seen in $\sigma(B)$ also produce an increase of $\kappa(B)$, so the dip between peaks in $\kappa(B)$ is filled in and we observe a single broader peak.

For higher temperatures the role played by the second term of Eq. (12) further increases and $\kappa(B)$ and $\kappa_0(B)$ behave quite differently. Finally we observe the above-mentioned picture when at $T=28$ K the oscillations of $\sigma(B)$ are damped. One can still see some oscillations of $\kappa(B)$, but the positions of the peaks do not coincide with the positions of the peaks in $\sigma(B)$ and $\kappa(B)$ observed at lower temperatures.

(vi) The behavior of Lorenz number is shown in Fig. 5. Since in the chosen temperature interval the inequality $T \ll \mu$ is well justified, we observe that the WF law is maintained in zero field (see Ref. 26). In nonzero field we observe violations of the WF law that become stronger as the temperature increases. At $T=3$ K the behavior of $L(B)$ is similar to the behavior of $\kappa_0(B)$ and two satellite peaks in $L(B)$ are related to the broad peak in $\kappa(B)$, while the dip between these peaks is caused by the peak of $\sigma(B)$. As the temperature increases, a more complicated behavior of $\kappa(B)$ results in the large-amplitude oscillations of $L(B)$. The positions of the peaks are not related to the positions of low-$T$ SdH oscillations. In the high-field regime $B>10$ T there is a tendency to the restoration of the WF law.

The above-presented picture is already quite complicated due to the interplay between the first and second terms of Eq. (12) so that in general there are no correlations between the low-temperature SdH oscillations and oscillations in $\kappa(B)$ and $L(B)$ seen at higher temperatures. Further complications can be caused by the fact that the impurity scattering rate $\Gamma$ which we assumed to be field and temperature independent may, in fact, depend on both $B$ and $T$.[29,30]

Let us now discuss the relation of the obtained theoretical results to the experiments.[8,11,12] To compare the results for electrical conductivity shown in Fig. 2, one should bear in mind the difference between graphene and graphite mentioned in item 2. In Ref. 8 the measurements were done at $T=2$ K and the oscillations are clearly seen and some of them, as stated in Ref. 8, are related to the quasiparticles with a linear dispersion. It is likely that for higher temperatures the oscillations of $\sigma(B)$ are suppressed[11] and we also see that at $T=28$ K the oscillations of $\sigma(B)$ are practically smeared out.

A comparison with experimental results for thermal conductivity is more complicated because the measured thermal conductivity $\kappa_{\text{exp}}(B,T) = \kappa(B,T) + \kappa_{\text{ph}}(B,T)$ besides the electron contribution, $\kappa(B,T)$ contains also the contribution from phonons, $\kappa_{\text{ph}}(T)$, which is assumed to be field independent. Accordingly, we can relate theoretically calculated $\kappa(B,T)/\kappa(B=0,T)$ shown in Fig. 3 with the experimentally accessible ratio $\kappa_{\text{exp}}(B,T)/\kappa_{\text{exp}}(B=0,T)$ via

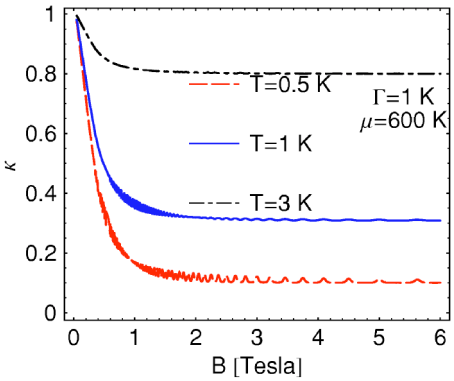


FIG. 6. (Color online) The normalized thermal conductivity $\kappa_{\text{exp}}(B,T)/\kappa_{\text{exp}}(B=0,T)$ [see Eq. (31)] as a function of field $B$ for three different values of temperature $T$ for $\mu=600$ K and $\Gamma=1$ K. We use $eB \to (4.5\times 10^4\ \text{K}^2)B$ (T) and $T_0=1.5$ K.

$$\frac{\kappa_{\text{expt}}(B,T)}{\kappa_{\text{expt}}(B=0,T)} = 1 + \frac{\kappa(B,T)/\kappa(B=0,T) - 1}{\kappa_{\text{ph}}(T)/\kappa(B=0,T) + 1} \approx 1 + \frac{\kappa(B,T)/\kappa(B=0,T) - 1}{(T/T_0)^2 + 1}. \quad (31)$$

The last equality is written using that the ratio $\kappa_{\text{ph}}(T)/\kappa(B=0,T)$ can be determined from the fact that at $T=T_0=1.5$ K the values $\kappa_{\text{ph}}(T_0) \sim \kappa(B=0,T_0)$,[12] so that assuming $\kappa_{\text{ph}}(T) \sim T^3$ and $\kappa(B=0,T) \sim T$ we estimate $\kappa_{\text{ph}}(T)/\kappa(B=0,T) \sim (T/T_0)^2$.

The ratio $\kappa_{\text{exp}}(B,T)/\kappa_{\text{exp}}(B=0,T)$ is plotted in Fig. 6. As one can see the MO's of $\kappa(B,T)$ are masked by the phonon contribution in $\kappa_{\text{exp}}(B,T)$ and only at rather low temperatures is there a possibility to observe them. Moreover, since the amplitude of MO's is higher for lower fields (see also Figs. 2–4), the MO's are more easily observable in the low-field regime.

Taking these facts into account, let us discuss the oscillations of thermal conductivity that were experimentally observed in Refs. 11 and 12 for $B \gtrsim 2$ Tesla. Since these oscillations are clearly seen only in the high-field regime and their amplitude increases as the field grows, their origin is unlikely to be related to the conventional SdH-like MO's and seems to be more associated with the quantum Hall effect. It would be interesting to check whether the conventional MO's of the electronic thermal conductivity $\kappa(B,T)$ predicted in this paper can be also observed in graphite when the measurements will be done at sufficiently low temperatures and/or the phonon contribution is subtracted.

## ACKNOWLEDGMENT

We gratefully acknowledge P. Esquinazi and A. Geim for helpful discussions.

*Electronic address: vgusynin@bitp.kiev.ua
†Present address: Bogolyubov Institute for Theoretical Physics, Kiev, Ukraine. Electronic address: sharapov@bitp.kiev.ua

[1] A. A. Abrikosov, Phys. Rev. B **58**, 2788 (1998).
[2] D. Shoenberg, *Magnetic Oscillations in Metals* (Cambridge University Press, Cambridge, England, 1984).
[3] G. P. Mikitik and Yu. V. Sharlai, Phys. Rev. Lett. **82**, 2147 (1999).
[4] S. G. Sharapov, V. P. Gusynin, and H. Beck, Phys. Rev. B **69**, 075104 (2004).
[5] R. Saito, G. Dresselhaus, and M. S. Dresselhaus, *Physical Properties of Carbon Nanotubes* (Imperial College Press, London, 1998).
[6] Y. Kopelevich, P. Esquinazi, J. H. S. Torres, R. R. da Silva, H. Kempa, F. Mrowka, and R. Ocana, *Studies of High Temperature Superconductors* (Nova Science Publishers Inc., New York, 2003), Vol. 45, pp. 59–106.
[7] G. Dresselhaus, Phys. Rev. B **10**, 3602 (1974).
[8] I. A. Luk'yanchuk and Y. Kopelevich, Phys. Rev. Lett. **93**, 166402 (2004).
[9] S. Uji, J. S. Brooks, and Y. Iye, Physica B **246-247**, 299 (1998).
[10] Z. M. Wang, Q. Y. Xu, G. Ni, and Y. W. Du, Phys. Lett. A **314**, 328 (2003).
[11] R. Ocaña, P. Esquinazi, H. Kempa, J. H. S. Torres, and Y. Kopelevich, Phys. Rev. B **68**, 165408 (2003).
[12] K. Ulrich and P. Esquinazi, J. Low Temp. Phys. **137**, 217 (2004).
[13] T. Matsui, H. Kambara, Y. Niimi, K. Tagami, M. Tsukada, and H. Fukuyama, cond-mat/0405011 (unpublished).
[14] K. S. Novoselov, A. K. Geim, S. V. Morozov, D. Jiang, Y. Zhang, S. V. Dubonos, I. V. Grigorieva, and A. A. Firsov, Science **306**, 666 (2004).
[15] K. S. Novoselov, A. K. Geim, S. V. Morozov, S. V. Dubonos, Y. Zhang, and D. Jiang, cond-mat/0410631 (unpublished).
[16] G. W. Semenoff, Phys. Rev. Lett. **53**, 2449 (1984).
[17] J. Gonzàlez, F. Guinea, and M. A. H. Vozmediano, Nucl. Phys. B **406**, 771 (1993); Phys. Rev. B **63**, 134421 (2001).
[18] D. V. Khveshchenko, Phys. Rev. Lett. **87**, 246802 (2001).
[19] E. V. Gorbar, V. P. Gusynin, V. A. Miransky, and I. A. Shovkovy, Phys. Rev. B **66**, 045108 (2002).
[20] T. Tokumoto, E. Jobiliong, E. S. Choi, Y. Oshima, and J. S. Brooks, Solid State Commun. **129**, 599 (2004).
[21] X. Du, S.-W. Tsai, D. L. Maslov, and A. F. Hebard, cond-mat/0404725 (unpublished).
[22] C. Thomsen and S. Reich, Phys. Rev. Lett. **85**, 5214 (2000).
[23] V. P. Gusynin, V. A. Miransky, and I. A. Shovkovy, Phys. Rev. Lett. **73**, 3499 (1994); Phys. Rev. D **52**, 4718 (1995).
[24] Y. Kopelevich, J. H. S. Torres, R. R. da Silva, F. Mrowka, H. Kempa, and P. Esquinazi, Phys. Rev. Lett. **90**, 156402 (2003).
[25] G. D. Mahan, *Many-Particle Physics* (Plenum, New York, 1990).
[26] S. G. Sharapov, V. P. Gusynin, and H. Beck, Phys. Rev. B **67**, 144509 (2003).
[27] E. J. Ferrer, V. P. Gusynin, and V. de la Incera, Eur. Phys. J. B **33**, 397 (2003).
[28] R. E. Prange, *The Quantum Hall Effect*, edited by R. E. Prange and S. M. Girvin (Springer-Verlag, New York, 1987).
[29] T. Champel and V. P. Mineev, Phys. Rev. B **66**, 195111 (2002); **67**, 089901(E) (2003).
[30] P. D. Grigoriev, Phys. Rev. B **67**, 144401 (2003).
[31] P. L. Taylor, *A Quantum Approach to the Solid State* (Prentice-Hall, Englewood Cliffs, 1970).